ELSEVIER

Comput. Methods Appl. Mech. Engrg. 191 (2001) 861–877

Computer methods in applied mechanics and engineering

www.elsevier.com/locate/cma

# Averaging technique for a posteriori error control in elasticity. Part III: Locking-free nonconforming FEM

Carsten Carstensen [1], Stefan A. Funken *

*Mathematisches Seminar, Christian-Albrechts-Universität zu Kiel, Ludewig-Meyn-Strasse 4, D-24098 Kiel, Germany*

Received 1 March 2000; received in revised form 14 September 2000

**Abstract**

In the third part of our investigations on averaging techniques for a posteriori error control in elasticity we focus on nonconforming finite elements in two dimensions. Kouhia and Stenberg [Comput. Methods Appl. Mech. Engrg. 124 (1995) 195] established robust a priori error estimates for a Galerkin-discretisation where the first component of the discrete displacement function is discretised with conforming and the second with nonconforming $P1$ finite elements. Here we study robust, i.e., $\lambda$-independent reliability and efficiency estimates for averaging error estimators. Numerical evidence supports that the reliability depends on the smoothness of given right-hand sides and independent of the structure of a shape-regular mesh. 

*Keywords:* Elasticity; A posteriori error estimates; Adaptive algorithm; Reliability; Finite element method; Nonconforming finite elements

## 1. Introduction

For a Poisson ratio $\nu$ close to 1/2, the Lamé constant $\lambda$ is very large and dominates the Navier–Lamé equations

$$(\lambda+\mu)\nabla \operatorname{div} u + \mu\Delta u = f, \tag{1.1}$$

the standard model of homogeneous isotropic linear elastic materials. In a conforming finite element analysis, the poor approximation of $\lambda \operatorname{div}(u-u_h)$ leads to (quasi-optimal) error estimates in which the large parameter $\lambda$ enters and causes a poor convergence in the energy norm. Although the convergence rate is optimal, the multiplicative factor is that large that the entire finite element approximation is pointless unless one refines unreasonably high.

Mixed and nonconforming finite element methods have been proposed to remedy this locking phenomenon such as PEERS or conforming–nonconforming schemes. We refer to [3,17,19] for background information on these finite element techniques and their a priori error analysis. To the best of our knowledge, in the rapidly developing field of a posteriori error analysis, only [6,7] provide robust error control for a finite element discretisation of (1.1) in the sense that $\lambda$ may explicitly arise in the error norm $E$

* Corresponding author. Current address: Mathematisches Institut, Universität Erlangen-Nürnberg, Bismarckstrasse 1 1/2, D-91054 Erlangen, Germany.

*E-mail addresses:* carsten.carstensen@tuwien.ac.at (C. Carstensen), funken@mi.uni-erlangen.de (S.A. Funken).

[1] Current address: Institute for Applied Mathematics and Numerical Analysis, Vienna University of Technology, Wiedner Hauptstrasse 8-10, A-1040 Vienna, Austria.

0045-7825/01/$ - see front matter 
PII: S0045-7825(01)00202-X

as well as in the (computable) error indicator $\eta$ but does not affect the constants $c_1$ and $c_2$ in the reliability estimate $E \leqslant c_1\eta$ and efficiency estimate $\eta \leqslant c_2 E + \text{h.o.t.}$

Nonconforming finite element schemes are much more established for fluid dynamics than for elasticity and so is their a posteriori error analysis [1,9]. Therefore, we first establish reliability and efficiency for residual-based error estimates $\eta = \eta_R^2 := (\sum_{T\in\mathscr{T}} \eta_{R,T}^2)^{1/2}$ with the local error indicators $\eta_{R,T}$

$$\eta_{R,T}^2 := \|h_{\mathscr{T}} f\|_{L^2(T)}^2 + \|h_{\mathscr{E}}^{1/2}[\sigma_h \cdot n_{\mathscr{E}}]\|_{L^2(\partial T)}^2 + \|h_{\mathscr{E}}^{1/2}[\partial u_h/\partial s]\|_{L^2(\partial(T)}^2 \tag{1.2}$$

for the element $T \in \mathscr{T}$. In case $f$ is (globally) smooth, we even improve this estimate by replacing $\|h_{\mathscr{T}} f\|_{L^2(T)}$ in (1.2) by the higher-order term $\|h_{\mathscr{T}}^2 Df\|_{L^2(T)}$. While the jumps of the discrete stress vectors on interior edges $\|h_E^{1/2}[\sigma_h \cdot n_E]\|_{L^2(E)}$ are well established, the nonconforming error $\|h_E^{1/2}[\partial u_h/\partial s]\|_{L^2(E)}$ quantifies the lack of continuity along the edge $E$ with the derivative $\partial/\partial s$ with respect to the arc-length as in [2,4,14]. For the Laplace equation the two jump terms together read $\|h_E^{1/2}[Du_h]\|_{L^2(E)}$ and owing to local equivalences of norms, averaging techniques can be justified on the basis of $\eta_R$ as in [5]. For the elasticity problem (1.1) at hand, the two jump contributions measure different residuals, namely equilibrium and compatibility of displacement and strain. Consequently, we face an estimator $\eta = \eta_Z + \eta_u + \text{h.o.t}$ (the higher-order terms, h.o.t, are computable) with one stress-averaging term $\eta_Z$ from Parts I and II [10,11] plus an averaging term of the discrete gradient $D_{\mathscr{T}} u_h$ (not the discrete strains). It seems surprising that, for the lower-order nonconforming–conforming scheme [17] with a regular triangulation of the domain into triangles and a test space $\mathscr{V} = \mathscr{V}_1 \times \mathscr{V}_2$

$$\mathscr{V}_1 := \{V \in C(\Omega):\ V \text{ is affine on each } T \in \mathscr{T} \text{ and vanishes on } \Gamma_{\mathrm{D}}\}, \tag{1.3}$$

$$\mathscr{V}_2 := \{V:\ V \text{ is affine on each } T \in \mathscr{T},\ \text{continuous at midpoints of inner element boundaries, and vanishes at midpoints of edges } E \subset \Gamma_{\mathrm{D}}\} \tag{1.4}$$

(and modifications on $\Gamma_{\mathrm{D}}$, the Dirichlet boundary, for inhomogeneous boundary conditions for the discrete displacements), we can prove $\eta_u \leqslant c\eta_Z + \text{h.o.t.}$ and so establish robust reliable and efficient a posteriori error control for the stress averaging estimator

$$\eta_Z := \min_{\sigma^* \in \mathscr{Q}(\mathscr{T},g)} \|\sigma_h - \sigma^*\|_{L^2(\Omega)}. \tag{1.5}$$

This work investigates robust a posteriori error control general for conforming or nonconforming schemes and shows

$$E/c_1 \leqslant \eta \leqslant c_2 E + \text{h.o.t.} \tag{1.6}$$

The conforming–nonconforming scheme (1.3) and (1.4) is the natural choice as it is robust (bounded errors $E$ for $\lambda \to \infty$) and allows a robust a posteriori error estimation in the sense of (1.6). This paper is the third in a series initiated with Parts I and II [10,11] that analyses reliability of averaging techniques for a posteriori error control without any severe restriction on the meshes; the shape-regular finite element grid may be highly refined and locally nonsymmetric.

The outline of the remaining part of this paper is as follows. Notation and the results are provided in Section 2. Numerical experiments in Section 3 illustrate the robust behavior of the a priori error estimates of the nonconforming–conforming scheme. Proofs are given in Section 4.

## 2. Model example and results

The stress field $\sigma$ satisfies the equilibrium equations:

$$f + \operatorname{div}\sigma = 0 \quad \text{in } \Omega, \tag{2.1}$$

$$\sigma \cdot n = g \quad \text{on } \Gamma_{\mathrm{N}}, \tag{2.2}$$

for a given volume force $f \in L^2(\Omega)^2$ and an applied surface load $g \in L^2(\Gamma_{\mathrm{N}})^2$. The Lipschitz boundary $\Gamma = \partial\Omega$ of the plane body, occupied by a bounded domain $\Omega$ in $\mathbb{R}^2$, consists of a closed Dirichlet part $\Gamma_{\mathrm{D}}$

with positive surface measure and a remaining, relatively open and possibly empty, Neumann part $\Gamma_N := \Gamma \setminus \Gamma_D$. Suppose that $\Gamma_D$ is connected.

The Dirichlet data $u_D \in C(\Gamma_D)$ are supposed to be differentiable at any flat piece of $\Gamma_D$ such that the surface gradient is square-integrable (written $u_D \in H^1(\Gamma_D)$). Then, we suppose that the exact displacement field $u$ belongs to $H^1(\Omega)^2$, i.e., $u \in L^2(\Omega)^2$ and the gradient $Du$ satisfies $Du \in L^2(\Omega)^{2\times 2}$, and satisfies

$$u = u_D \quad \text{on } \Gamma_D. \tag{2.3}$$

The linear Green strain tensor $\varepsilon(u) := \operatorname{sym} Du = \frac{1}{2}(u_{j,k} + u_{k,j})_{j,k=1,2}$ is linearly related to the stress $\sigma$,

$$\sigma = \mathbb{C}\varepsilon(u) \quad \text{in } \Omega. \tag{2.4}$$

The two positive Lamé constants $\lambda$ and $\mu$ play different roles in the material law

$$\mathbb{C}\tau = \lambda \operatorname{tr}(\tau)\mathbb{1}_{2\times 2} + 2\mu\tau \quad \text{for all } \tau \in \mathbb{R}^{d\times d}_{\text{sym}}. \tag{2.5}$$

While $\mu$ is fixed we carefully analyze $\lambda \to \infty$ in the material law (2.5) and denote the dependence of $\lambda$ explicitly in the notation.

There exists exactly one (weak) solution $u \in H^1(\Omega)^2$ to (2.1)–(2.4) which is approximated by a finite element method on a mesh $\mathcal{T}$. We suppose that $\mathcal{T}$ is a regular triangulation of $\Omega \subset \mathbb{R}^2$ in the sense of Ciarlet [13], i.e., $\mathcal{T}$ is a finite partition of $\Omega$ in closed triangles or parallelograms; two distinct elements $T_1$ and $T_2$ in $\mathcal{T}$ are either disjoint or $T_1 \cap T_2$ is a complete edge or a common node of both $T_1$ and $T_2$. With $\mathcal{T}$ let $\mathcal{E}$ denote the set of all edges, and we assume that $E \in \mathcal{E}$ either belongs to $\Gamma_D$ or $E \cap \Gamma_D$ has vanishing surface measure, so there is no change of boundary conditions within one edge $E \subseteq \Gamma$. Furthermore, let $P_k(T)$, respectively, $Q_k(T)$ denote the set of algebraic polynomials of total respective partial degree $\leqslant k$ and define $\mathcal{P}_k(T) := \mathcal{P}_k(T)$ if $T$ is a triangle and $P_k(T) := Q_k(T)$ if $T$ is a parallelogram.

Then, the finite element solution $u_h$ is supposed to be smooth on each triangle, e.g., $u_h \in H^2(\mathcal{T})^2$, but may be discontinuous at inner element boundaries. Consequently, the distributional derivatives of $u_h$ may involve Dirac measures on edges and are different from their $\mathcal{T}$-elementwise application which we will denote differently by the subindex $\mathcal{T}$, e.g., $\varepsilon_{\mathcal{T}}(u)$ or $\operatorname{div}_{\mathcal{T}} u$ defined by $\varepsilon_{\mathcal{T}}(u) = \varepsilon(u|_T)$ on each element $T \in \mathcal{T}$.

Despite the (possibly) discontinuous approximation $u_h$ we suppose that amongst the test functions in the weak form of the equilibrium condition are continuous $\mathcal{T}$-piecewise affine, i.e., we assume

$$\int_\Omega \varepsilon(v_h) : \mathbb{C}\varepsilon_{\mathcal{T}}(u_h)\,dx = \int_\Omega f \cdot v_h\,dx + \int_{\Gamma_N} g \cdot v_h\,ds \tag{2.6}$$

holds for all test functions $v_h \in \mathcal{S} := \mathcal{S}_1(\mathcal{T})^2 \cap H^1_D(\Omega)$.

The Lebesgue and Sobolev spaces $L^2(\Omega)$ and $H^1(\Omega)$ are defined as usual [16,18] and

$$\begin{aligned}
&\mathcal{L}_k(\mathcal{T}) := \{V \in L^\infty(\bar\Omega) : \forall T \in \mathcal{T},\ V|_T \in \mathcal{P}_k(T)\},\\
&\mathcal{S}_1(\mathcal{T}) := \mathcal{L}_1(\mathcal{T}) \cap C(\bar\Omega),\\
&H^1_D(\Omega) := \{v \in H^1(\Omega)^2 : v|_{\Gamma_D} = 0\},\\
&H^k(\Omega) := \{v \in L^2(\Omega) : \partial^{|\alpha|} v/\partial x^\alpha \in L^2(\Omega) \text{ for all multiindices } \alpha \text{ with } |\alpha| \leqslant k\},\\
&H^k(\mathcal{T}) := \{v \in L^2(\Omega) : \forall T \in \mathcal{T},\ v|_T \in H^k(T)\}.
\end{aligned}$$

Given $u_h$ let $\sigma_h := \mathbb{C}\varepsilon_{\mathcal{T}}(u_h)$ and let $[\cdot]$ denote the jumps across edges. For the discrete stress, $[\sigma_h]n_{\mathcal{E}}$ is defined on the skeleton $\bigcup \mathcal{E}$ along the edge $E \in \mathcal{E}$ as $[\sigma_h]n_{\mathcal{E}} = 0$ if $E \subset \Gamma_D$, as $[\sigma_h n_E] := g - \sigma_h n$ if $E \subset \bar\Gamma_N$, and as $[\sigma_h]n_{\mathcal{E}} = (\sigma_h|_{T_+} - \sigma_h|_{T_-})n_{\mathcal{E}}$ on an interior edge $T_+ \cap T_- = E,\ T_\pm \in \mathcal{T}$. For the displacements, the derivative along $E \in \mathcal{E}$ is given by $\partial \cdot / \partial s$ and $[\partial u_h/\partial s]$ denotes the difference of the traces at $E = T_+ \cap T_-$ of the tangential derivatives of $u_h$ in $T_+$ and $T_-$. If $E \subset \Gamma_D$ belongs to the Dirichlet part of the boundary, then $[\partial u_h/\partial s] := \partial(u_D - u_h)/\partial s$. If $E \subset \bar\Gamma_N$ belongs to the Neumann part of the boundary, then $[\partial u_h/\partial s] := 0$. To stress that the derivatives along $\bigcup \mathcal{E}$ are understood edgewise, we write $[\partial_{\mathcal{E}} u_h/\partial s]$ for them.

The first result is a standard residual a posteriori error estimate; all proofs will be given in Section 4.

**Theorem 2.1.** *Let $u \in H^1(\Omega)^2$ solve (2.1)–(2.4) and let $u_h \in H^2(\mathscr{T})^2$ satisfy (2.6). Suppose $f \in L^2(\Omega)^2$ and $g \in L^2(\Gamma_N)^2$. Then*

$$\begin{aligned}&\|2\mu\varepsilon_{\mathscr{T}}(u-u_h)\|_{L^2(\Omega)} + \|\lambda \mathrm{div}_{\mathscr{T}}(u-u_h)\|_{L^2(\Omega)}\\ &\quad\leqslant c_3\Big(\|h_{\mathscr{T}}(f+\mathrm{div}_{\mathscr{T}}\sigma_h)\|_{L^2(\Omega)} + \|h_{\mathscr{E}}^{1/2}[\sigma_h]n_{\mathscr{E}}\|_{L^2\left(\bigcup\mathscr{E}\right)} + \|h_{\mathscr{E}}^{1/2}[\partial_{\mathscr{E}}u_h/\partial s]\|_{L^2\left(\bigcup\mathscr{E}\right)}\Big).\end{aligned} \tag{2.7}$$

*The $(h_{\mathscr{T}}, h_{\mathscr{E}}, \lambda)$-independent constant $c_3 > 0$ depends on the shape of the elements and patches only.*

In case $\mathrm{div}_{\mathscr{T}}\sigma_h = 0$, e.g., for lowest-order schemes, the edge contributions dominate.

**Theorem 2.2.** *Let $u \in H^1(\Omega)^2$ solve (2.1)–(2.4) and let $u_h \in \mathscr{L}^1(\mathscr{T})^2$ satisfy (2.6). Suppose $f \in H^1(\Omega)^2$ and $g \in L^2(\Gamma_N)^2$. Then*

$$\begin{aligned}&\|2\mu\varepsilon_{\mathscr{T}}(u-u_h)\|_{L^2(\Omega)} + \|\lambda \mathrm{div}_{\mathscr{T}}(u-u_h)\|_{L^2(\Omega)}\\ &\quad\leqslant c_4\Big(\|h_{\mathscr{E}}^{1/2}[\sigma_h]n_{\mathscr{E}}\|_{L^2\left(\bigcup\mathscr{E}\right)} + \|h_{\mathscr{E}}^{1/2}[\partial_{\mathscr{E}}u_h/\partial s]\|_{L^2\left(\bigcup\mathscr{E}\right)} + \|h_{\mathscr{T}}^2 Df\|_{L^2(\Omega)}\Big).\end{aligned} \tag{2.8}$$

*The $(h_{\mathscr{T}}, h_{\mathscr{E}}, \lambda)$-independent constant $c_4 > 0$ depends on the shape of the elements and patches only.*

**Remark 2.1.** (i) The residual-based a posteriori error estimates (2.16) and (2.8) are efficient in the sense of (1.6). (For a proof, cf., e.g. [9] and below.)

(ii) One drawback of the estimate in (2.16) and (2.8) is the presence of constants whose strict estimation could result in a huge overestimation (of a factor 20–30, cf. [8]).

(iii) The aim of this paper is the analysis of averaging techniques since there is an obvious choice of a constant $c_2 = 1$ from the efficiency estimate.

Compared to conforming schemes, the equilibrium and compatibility errors give rise to two averaging processes. Let $\mathscr{E}_N$ denote the edges on the Neumann boundary and recall from Part I [10]

$$\mathscr{Q}(\mathscr{T}, g) := \{\sigma^* \in \mathscr{S}^1(\mathscr{T})^{2\times 2}\colon \sigma^*(z)\cdot n_E = g(z) \text{ for all } z \in \mathscr{N}\cap E \text{ with } E \in \mathscr{E}_N\}, \tag{2.9}$$

which requires some continuity on $g$: At those nodes $z$ on $\Gamma_N$, where $\Gamma_N$ is flat and so the normal vectors coincide $n_{E_1} = n_{E_2}$ for two distinct neighboring $E_1, E_2 \in \mathscr{E}_N$, the continuity of $\sigma^*$ at $z \in E_1 \cap E_2 \cap \mathscr{N}$ implies that the restrictions $g|_{E1}$ and $g|_{E2}$ coincide at $z$. Note that $\mathscr{Q}(\mathscr{T}, g) = \mathscr{S}^1(\mathscr{T})^{2\times 2}$ in the case of pure Dirichlet conditions. Then

$$\eta_Z := \min_{\sigma^*\in\mathscr{Q}(\mathscr{T},g)} \|\sigma_h - \sigma^*\|_{L^2(\Omega)} \tag{2.10}$$

is a lower bound of each averaging estimator (up to the Neumann boundary conditions). Similarly, let $t_{\mathscr{E}}$ denote the tangential unit vector along $\Gamma$ and define

$$\eta_u := \min_{Q\in S^1(\mathscr{T})^{2\times 2}} \left(\|D_{\mathscr{T}}u_h - Q\|_{L^2(\Omega)} + \left\|h_{\mathscr{E}}^{1/2}\left(\frac{\partial u_D}{\partial s} - Qt_{\mathscr{E}}\right)\right\|_{L^2(\Gamma_D)}\right). \tag{2.11}$$

**Theorem 2.3.** *Let $u \in H^1(\Omega)^2$ solve (2.1)–(2.4) and let $u_h \in H^2(\mathscr{T})^2$ satisfy (2.6). Suppose $f \in L^2(\Omega)^2$ and $g \in L^2(\Gamma_N)$. Then*

$$\begin{aligned}\eta_Z - \min_{\sigma^*\in\mathscr{Q}(\mathscr{T},g)} \|\sigma - \sigma^*\|_{L^2(\Omega)} &\leqslant \|2\mu\varepsilon_{\mathscr{T}}(u-u_h)\|_{L^2(\Omega)} + \|\lambda \mathrm{div}_T(u-u_h)\|_{L^2(\Omega)}\\ &\leqslant c_5\Big(\eta_Z + \eta_u + \|h_{\mathscr{E}}^{3/2}\partial_{\mathscr{E}}^2 u_D/\partial s^2\|_{L^2(\Gamma_D)} + \|h_{\mathscr{T}}^2 Df\|_{L^2(\Omega)} + \|h_{\mathscr{E}}^{3/2}\partial_{\mathscr{E}}g/\partial s\|_{L^2(\Gamma_N)}\Big).\end{aligned} \tag{2.12}$$

*The $(h_{\mathscr{T}}, h_{\mathscr{E}}, \lambda)$-independent constant $c_5 > 0$ depends on the shape of the elements and patches only.*

It is clear that $\eta_u$ is efficient. By choosing $Q$ as an approximation to the exact displacement gradient $Du$ and a triangle inequality, we have

$$\begin{aligned}\eta_u &\leqslant \|D_{\mathscr{T}} u_h - Q\|_{L^2(\Omega)} + \left\| h_{\mathscr{E}}^{1/2} \left( \frac{\partial u_{\mathrm{D}}}{\partial s} - Q t_{\mathscr{E}} \right) \right\|_{L^2(\Gamma_{\mathrm{D}})} \\ &\leqslant \|D_{\mathscr{T}}(u_h - u)\|_{L^2(\Omega)} + \|Du - Q\|_{L^2(\Omega)} + \|h_{\mathscr{E}}^{1/2}(Du - Q)t_{\mathscr{E}})\|_{L^2(\Gamma_{\mathrm{D}})}, \end{aligned} \tag{2.13}$$

and the last two terms are of higher order if $u$ is smooth.

Moreover, we show that $\eta_u$ can be neglected in (2.12) in case of the conforming–nonconforming scheme (1.3) and (1.4) from [17]. To involve nonhomogeneous Dirichlet data, suppose that $u_h$ belongs to $\mathscr{W} = \mathscr{W}_1 \times \mathscr{W}_2$ where the jumps on inner element edges or Dirichlet edges that satisfy different continuity conditions in each component

$$\mathscr{W}_1 := \{w_h \in \mathscr{L}_1(\mathscr{T})\colon \forall E \in \mathscr{E},\ [w_h] \text{ vanishes at the endpoints of } E\}, \tag{2.14}$$

$$\mathscr{W}_2 := \left\{ w_h \in \mathscr{L}_1(\mathscr{T})\colon \forall E \in \mathscr{E},\ \int_E [w_h]\,\mathrm{d}s = 0 \right\}; \tag{2.15}$$

the jump at boundary edges is understood as $[w_h] := 0$ on $\Gamma_{\mathrm{N}}$ and $[w_h] := u_{\mathrm{D}} - w_h$ on $\Gamma_{\mathrm{D}}$.

Certain triangulations are excluded which normally yield a singular discrete problem and are hence in practice avoided anyway: Suppose $\mathscr{E}_{\mathrm{D}}$ consists of at least two edges and that each edge $E \not\subset \Gamma$ which is parallel to the $x_1$-axis has at least one endpoint which does not belong to the boundary too.

The subsequent a posteriori estimate (2.16) states reliability as in (1.6). The efficiency in (1.6) follows from Theorem 2.3.

**Theorem 2.4.** *Let $u \in H^1(\Omega)^2$ solve (2.1)–(2.4) and let $u_h \in \mathscr{W}_1 \times \mathscr{W}_2$ satisfy (2.6). Suppose $f \in H^1(\Omega)^2$ and $g \in H^1(\mathscr{E}_{\mathrm{N}})^2$ and $u_{\mathrm{D}} \in C(\Gamma_{\mathrm{D}}) \bigcup H^1(\Gamma_{\mathrm{D}})$ belongs to $H^2(\gamma)$ for each edge $\gamma$ of the polygon $\Gamma_{\mathrm{D}}$. Then*

$$\begin{aligned}&\|2\mu\varepsilon_{\mathscr{T}}(u - u_h)\|_{L^2(\Omega)} + \|\lambda \mathrm{div}_{\mathscr{T}}(u - u_h)\|_{L^2(\Omega)} \\ &\quad\leqslant c_6 \Big( \eta_Z + \|h_{\mathscr{E}}^{3/2} \partial_{\mathscr{E}}^2 u_{\mathrm{D}}/\partial s^2\|_{L^2(\Gamma_{\mathrm{D}})} + \|h_{\mathscr{E}}^{3/2} \partial_{\mathscr{E}} g/\partial s\|_{L^2(\Gamma_{\mathrm{D}})} + \|h_{\mathscr{T}}^2 Df\|_{L^2(\Omega)} \Big). \end{aligned} \tag{2.16}$$

*The $(h_{\mathscr{T}}, h_{\mathscr{E}}, \lambda)$-independent constant $c_6 > 0$ depends on the shape of the elements and patches only.*

Instead of $\eta_Z$ we calculate $\eta_{\mathscr{A}} := \|\sigma_h - \mathscr{A}\sigma_h\|_{L^2(\Omega)}$ with the averaging operator $\mathscr{A}$ based on a function $\sigma_h^* \in \mathscr{S}^1(\mathscr{T})^{2\times 2}$ which satisfies $g(z) = \sigma_h^*(z) n_E(z)$ for each endpoint $z$ of an edge $E$ on $\bar{\Gamma}_{\mathrm{N}}$. We define

$$\mathscr{A}\sigma_h := \sigma_h^* := \sum_{z \in \mathscr{N}} \mathscr{I}_z(\sigma_h)\varphi_z, \tag{2.17}$$

where for $z \in \mathscr{N} \setminus \bar{\Gamma}_{\mathrm{N}} \mathscr{I}_z(\sigma_h) := \fint_{\omega_z} \sigma_h\,\mathrm{d}x$ is the integral mean of $\sigma_h$ over $\omega_z$, For $z \in \mathscr{N} \setminus \bar{\Gamma}_{\mathrm{N}}$ the discrete Neumann condition $g(z) = \sigma_h^*(z) n_E$ is taken into account by solving $4 \times 4$ linear system of equations. We refer to Part I [10] for computational details.

## 3. Numerical experiments

The three numerical experiments of Parts I and II [10,11] are complemented in this section with $L^2$-stress-error norms $e_{\mathrm{N}}$ and corresponding estimators $\eta_R$ and $\eta_{\mathscr{A}}$ for conforming–nonconforming finite element spaces. The following algorithm generated all meshes (perturbed for $\vartheta = 1$) of this paper and defines all quantities displayed in the examples below.

**Algorithm** $(A_{\mathscr{A}}^{\vartheta})$ (*resp.* $(A_R^{\vartheta})$).

(a) Start with coarse mesh $\mathscr{T}_0$, $k = 0$.

(b) Solve the discrete problem with respect to the actual mesh $\mathscr{T}_k$ with $N$ degrees of freedom and error $e_{\mathrm{N}} := \|\sigma - \sigma_h\|_{L^2(\Omega)}$.

(c) For Algorithm $(A^{\vartheta}_{\mathscr{A}})$ compute, for all $T \in \mathscr{T}_k$,

$$\eta_T = \eta_{\mathscr{A},T} := \|\sigma_h - \mathscr{A}\sigma_h\|_{L^2(T)}.$$

For Algorithm $(A^{\vartheta}_{R})$ compute, for all $T \in \mathscr{T}_k \eta_T = \eta_{R,T}$ as in with

$$\eta^2_{R,T} := \|h_{\mathscr{T}} f\|^2_{L^2(T)} + \|h^{1/2}_{\mathscr{E}}[\sigma_h \cdot n]\|^2_{L^2(\partial T)} + \mu^2 \|h^{1/2}_{\mathscr{E}}[\partial u_h/\partial s]\|^2_{L^2(\partial T)}.$$

(d) Compute a given stopping criterion based on $(\sum_{T\in\mathscr{T}_k} \eta^2_T)^{1/2}$, denoted $\eta_R$ resp. $\eta_{\mathscr{A}}$, and decide to terminate or to go to (e).
(e) Mark the element $T$ (*red* refinement) provided

$$\frac{1}{2} \max_{T'\in\mathscr{T}_k} \eta_{T'} \leqslant \eta_T.$$

(f) Mark further elements (*red–green–blue*-refinement) to avoid hanging nodes. Generate a new triangulation $\tilde{\mathscr{T}}_{k+1}$ using edge midpoints if $\vartheta = 0$ and points on the edges at a random distance at most $0.3h_E$ from the edge midpoints if $\vartheta = 1$. Perturb the nodes $z \in \mathscr{N}_{k+1}$ of the mesh $\tilde{\mathscr{T}}_{k+1}$ at random with values taken uniformly from a ball around $z$ of radius $\vartheta 2^{-k}/15$. Correct boundary nodes by orthogonal projection onto that boundary piece they are expected such that $\Omega$, $\Gamma_{\mathrm{D}}$, $\Gamma_{\mathrm{N}}$ are matched by the resulting mesh $\tilde{\mathscr{T}}_{k+1}$ exactly. Update $k$ and go to (b).

All examples concern the Navier–Lamé equation (1.1) in the form of (2.1)–(2.6) (cf. Part I [10, Subsection 4.1–4.3] for more details) and the conforming–nonconforming finite element scheme (1.3) and (1.4).

### 3.1. L-shaped domain with analytic solution

The model example on the L-shaped domain models singularities at re-entrant corners for Young's modulus $E = 100{,}000$ and the Poisson coefficient $0.3 \leqslant \nu < 0.5$. The considered exact solution is traction free, $g = 0$, on the Neumann boundary $\Gamma_{\mathrm{N}} := \mathrm{conv}\{(0,0),(-1,1)\} \bigcup \mathrm{conv}\{(0,0),(-1,-1)\}$ and $f = 0$.

Starting from the initial mesh $\mathscr{T}_0$ from Fig. 1 (top, left), we run Algorithm $(A^0_{\mathscr{A}})$. Here, in distinction to corresponding calculations in Parts I and II we use an initial mesh with twelve instead of six elements, because of the mild restrictions on the mesh (each edge $E \not\subset \Gamma$ has at least one endpoint which is an interior node). Fig. 1 shows a sequence of refined meshes from Algorithm $(A^1_{\mathscr{A}})$ $(\nu = 0.499)$ with

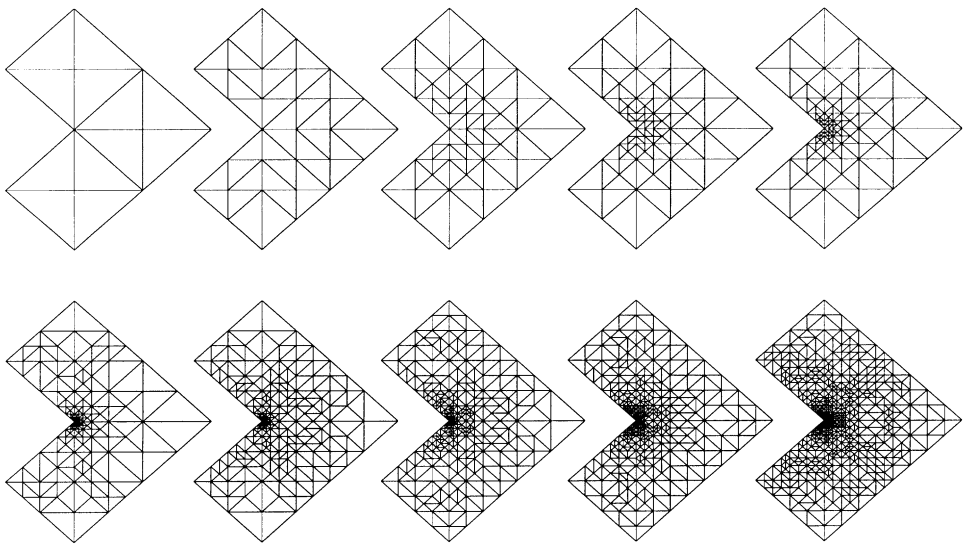

Fig. 1. $\mathscr{T}_0, \ldots, \mathscr{T}_9$ generated by Algorithm $(A^0_{\mathscr{A}})$ in Section 3.1.

optimal experimental convergence order 1. The resulting mesh after 11 adaptive refinements and a zoom at the re-entrant corner is shown in Fig. 2 and displays a rather high mesh-refinement near the singularity. All meshes are symmetric with respect to the $x$-axis and show a circular refinement around the origin. The shown meshes are similar to meshes shown in Part I [10, Subsection 4.1] for $\nu = 0.3$ and differ significantly from those given in Part II [11, Subsection 4.1] for $\nu = 0.499$; the adapted meshes for nonconforming finite element schemes appear stable as $\nu \to 0.5$ in contrast to the conforming scheme.

Errors $e_{\mathrm{N}}$ and error estimators $\eta_{\mathscr{A}}$, $\eta_R$ are displayed versus the number of degrees of freedom $N$ for $\nu = 0.3$ and 0.499 for uniform meshes and adaptively refined meshes generated by Algorithms $(A^0_{\mathscr{A}})$ resp. $(A^0_R)$ in Fig. 3.

The errors $e_{\mathrm{N}}$ and error estimators $\eta_{\mathscr{A}}$, $\eta_R$ have nearly the same magnitude for $\nu = 0.3$ and 0.499 and comparable $N$. This is experimental evidence for the robustness of the conforming–nonconforming finite element formulation.

For the sequences of uniform meshes we obtain experimentally convergence $\approx 0.54$ which coincides with the theoretically expected rate. (Note, $N \propto h^{-2}$ in two dimensions.) The adaptive mesh-refining Algorithm $(A^0_{\mathscr{A}})$ improves this experimental convergence order to 1 which is optimal for the used family of finite element spaces.

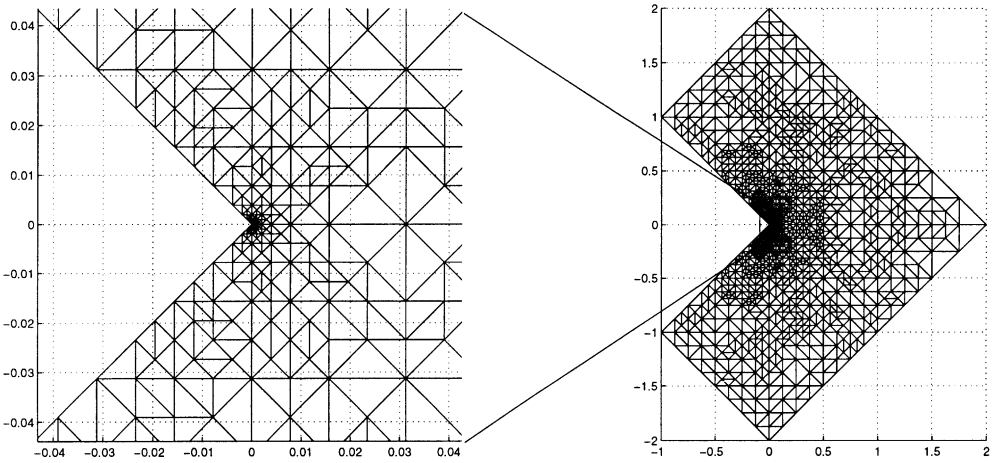


Fig. 2. Mesh $\mathscr{T}_{11}$ and magnified details at the re-entrant corner for Section 3.1 ($\nu = 0.499$).

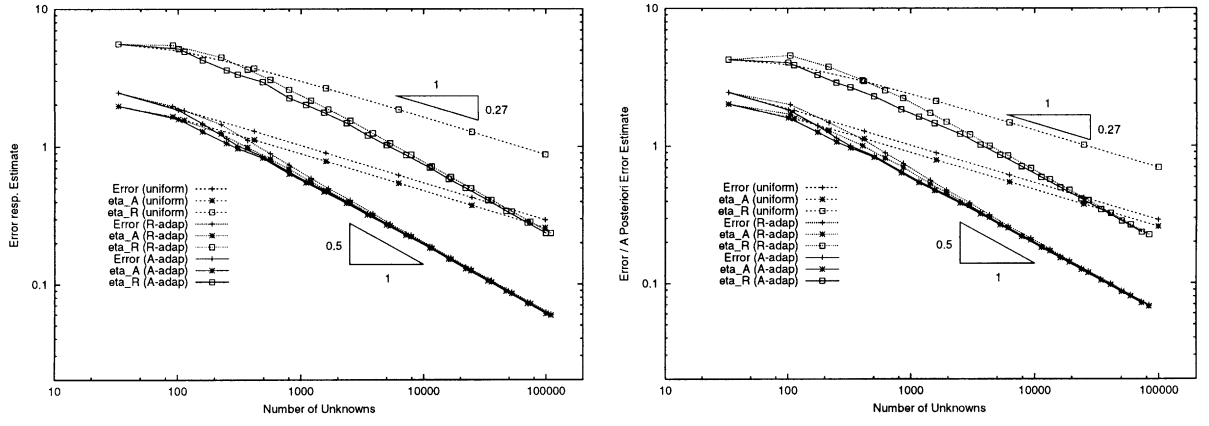


Fig. 3. Error indicators $\eta_{\mathscr{A}}$ and $\eta_R$ vs $N$ for uniform and adaptive meshes from Algorithms $(A^0_{\mathscr{A}})$ and $(A^0_R)$ of Section 3.1 ($\nu = 1/3$ left, $\nu = 0.499$ right.)

As in Parts I and II [10,11] we investigated experimentally whether super-convergence properties are responsible for the good performance of averaging techniques for a posteriori error control in practice. We take Algorithm $(A^1_{\mathscr{A}})$ to study the influence of local symmetries in the mesh; Algorithm $(A^1_{\mathscr{A}})$ perturbs the nodes in step (f). (We refer to [10] for a figure of a sequence of perturbed refined meshes from Algorithm $(A^1_{\mathscr{A}})$.)

For perturbed and nonperturbed meshes from Algorithm $(A^\vartheta_{\mathscr{A}})$ we display the extreme quotients of the error estimator $\eta_{\mathscr{A}}$ over the error $e_{\mathrm{N}} = \|\sigma - \sigma_h\|_{L^2(\Omega)}$ versus $1/2 - \nu$, i.e., the displayed constants are $\min\{\eta_A/e_{\mathrm{N}}\}$, and $\max\{\eta_A/e_{\mathrm{N}}\}$ for different values of $N$ corresponding to $\mathscr{T}_1, \ldots, \mathscr{T}_k$ for $k$ as implicitly shown in Fig. 3.

Fig. 4 shows that the reliability constant is bounded from above and the efficiency constant from below independently of the Poisson ratio $\nu$. This numerical experiment confirms numerically that the a posteriori error estimate is $h$-independent and supports that also for perturbed meshes the estimate (2.12) is reliable and efficient.

### 3.2. Cook's membrane problem

A tapered panel is clamped on the left end as depicted in Fig. 5 subject to a shearing load on the right end, i.e., $g = (0, 1000)$ on the right edge of $\Omega := \mathrm{conv}\{(0,0),(48,44),(48,60),(0,44)\}, g = 0$ on the

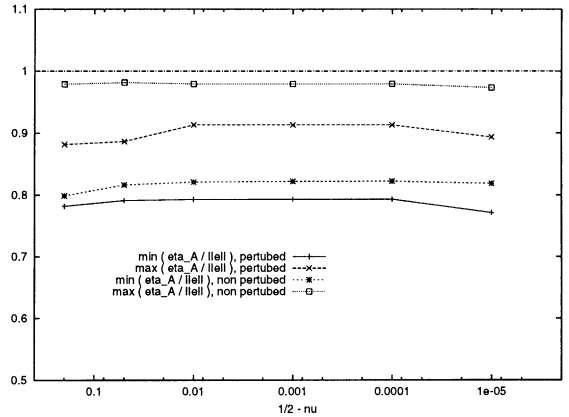


Fig. 4. Computed reliability/efficiency constants versus 1/2-$\nu$ for perturbed and nonperturbed meshes from Algorithm $(A^\vartheta_{\mathscr{A}})$ of Section 3.1.

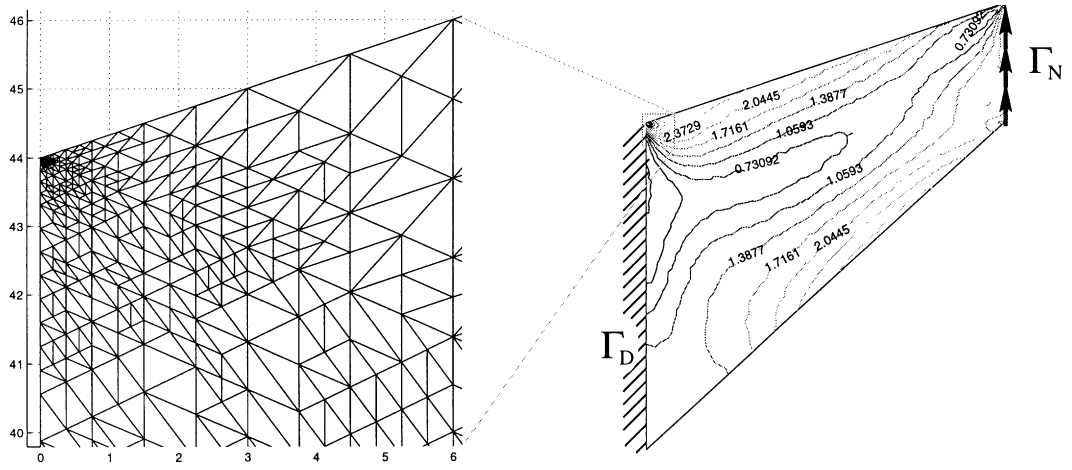


Fig. 5. Isolines of the approximated von Mises stress after 11 refinements generated by Algorithm $(A^0_{\mathscr{A}})$ and magnified detail at (0, 44) of Section 3.2 ($\nu = 0.499$).

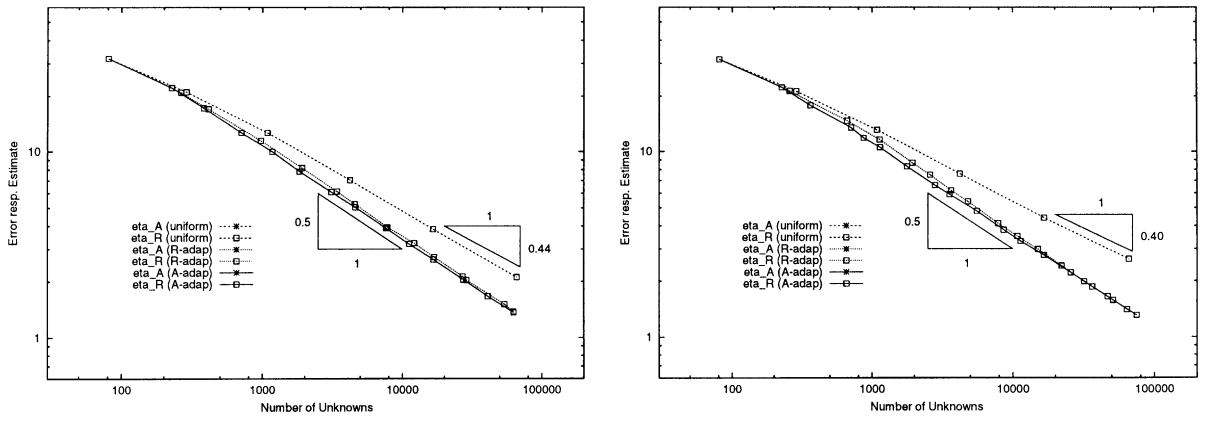


Fig. 6. Error indicators $\eta_{\mathscr{A}}$ and $\eta_R$ versus $N$ for uniform and adaptive meshes from Algorithms $(A^0_{\mathscr{A}})$ and $(A^0_R)$ of Section 3.2 ($v = 1/3$ left, $v = 0.499$ right.).

remaining part of $\Gamma_{\mathrm{N}}$, $u = 0$ on $\Gamma_{\mathrm{D}}$, and $f = 0$. The material constants are $E = 100{,}000$ and $v = 1/3$ or 0.499 and the initial mesh $\mathscr{T}_0$ is displayed in Fig. 6 (top, left).

A plot of $\mathscr{T}_{11}$ generated by Algorithm $(A^0_{\mathscr{A}})$ as some magnified details near the re-entrant corner (zoom of $(0,6) \times (40,46)$) is given in Fig. 5 for $v = 1/3$.

The a posteriori error estimates $\eta_{\mathscr{A}}$ and $\eta_R$ for $v = 0.3$ (left) and $v = 0.499$ (right) computed with uniform and adaptive refinements are given in Fig. 6.

The adaptive mesh-refining Algorithms $(A^0_Z)$ and $(A^0_R)$ yield a slope $-1/2$. Assuming that the error estimator $\eta_A$ is efficient and reliable as in Section 3.1 we obtain convergence order 1 which is asymptotically better than uniform refinement as observed in Fig. 6. For $v = 0.3$ and $v = 0.499$ corresponding graphs in Fig. 6 have nearly the same slope and magnitude which supports that the estimates are $(h_{\mathscr{T}}, h_{\mathscr{E}}, \lambda)$-independent.

A sequence of refined meshes generated by Algorithm $(A^1_{\mathscr{A}})$ $(v = 0.499)$ with optimal experimental convergence order 1 is shown in Fig. 7.

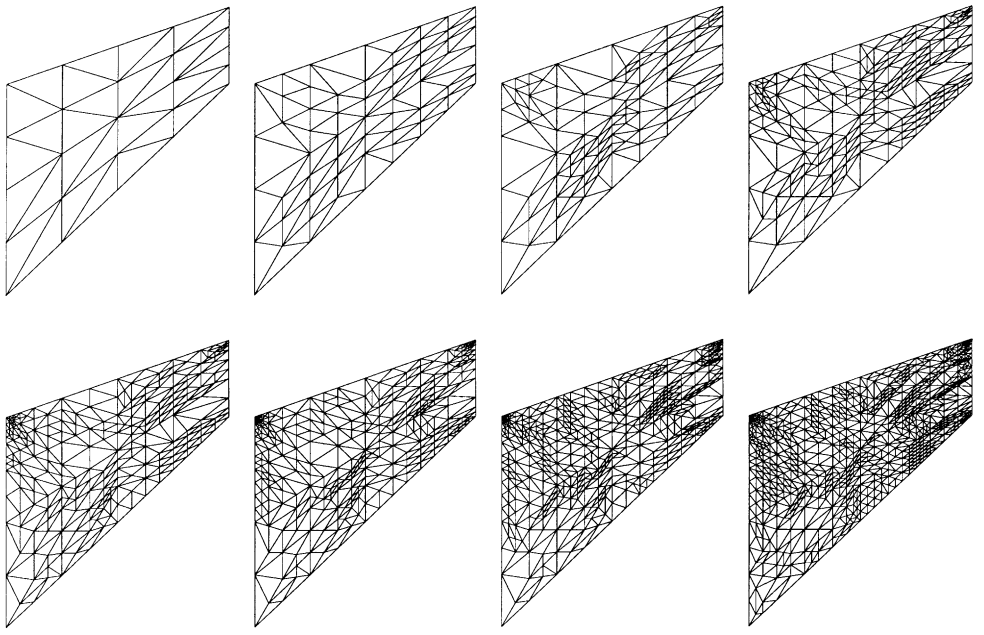

Fig. 7. $\mathscr{T}_0, \ldots, \mathscr{T}_7$ generated by Algorithm $(A^0_{\mathscr{A}})$ in Section 3.2 ($v = 0.3$).

### 3.3. Compact tension specimen

The compact tension specimen of Fig. 6 is loaded with a surface load $g = (0, 100)$ on $\Gamma_N = \{(x, y) \in \Gamma: |y| = 60\}$ and $f = 0$; $E = 100{,}000$ and $\nu = 0.3$ and 0.499. As the problem is symmetric, one half of the domain was discretised. We fixed the horizontal displacement with the constraint that the integral mean of all horizontal displacements is zero.

For coarse meshes, the problem behaves like a problem with re-entrant corner at $A = (50, 0)$ and hence we expect a higher mesh-refinement. The numerical solution for this problem with $\nu = 0.499$ and $N = 22{,}065$ and a magnification of the adaptively refined mesh around $(50, 0)$ is provided in Fig. 8. The a posteriori error estimates $\eta_{\mathcal{A}}$ and $\eta_R$ are plotted versus the number of degrees of freedom $N$ in Fig. 9. Assuming efficiency and reliability constants as computed in Section 3.1 we obtain optimal convergence rates 1 of $e_N$ for adaptive meshes. The experimental convergence rate of $\eta_{\mathcal{A}}$ and $\eta_R$ is approximately 1 for the adaptive meshes and (computed from the last two meshes) 0.5 resp. 0.27 for uniform meshes (see Fig. 10).

Both adaptive mesh-refining Algorithms $(A^0_{\mathcal{A}})$ and $(A^0_R)$ improve this experimental convergence order to the optimal order one. Similar as in Sections 3.1 and 3.2 corresponding graphs of the error estimators

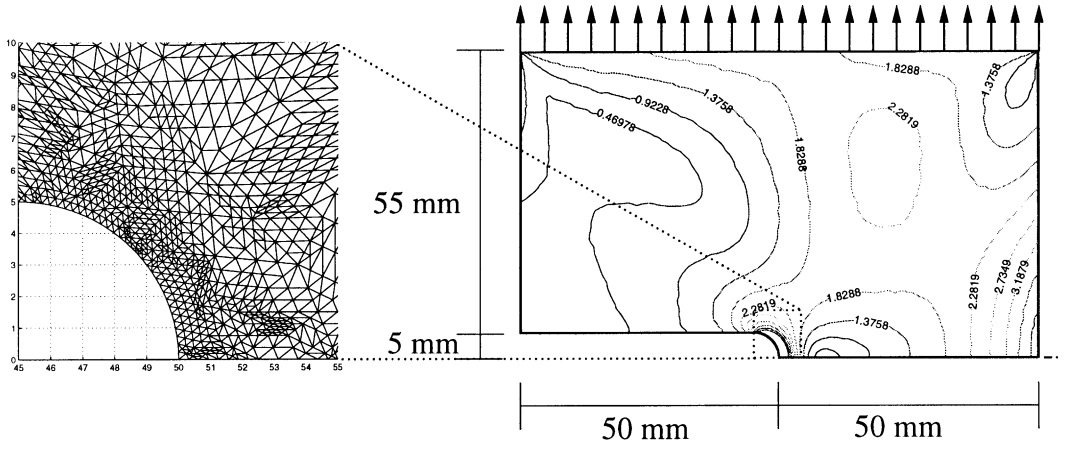


Fig. 8. Isolines of the approximated von-Mises stress after nine refinements generated by Algorithm $(A^0_{\mathcal{A}})$ and magnified details at $(50, 0)$ of Section 3.3 ($\nu = 0.499$).

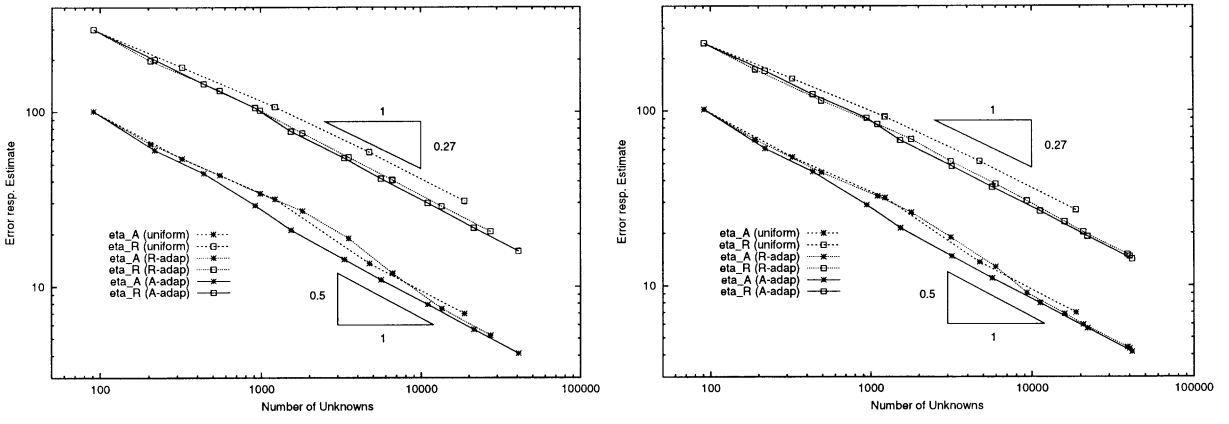


Fig. 9. Error indicators $\eta_{\mathcal{A}}$ and $\eta_R$ versus $N$ for uniform and adaptive meshes from Algorithms $(A^0_{\mathcal{A}})$ and $(A^0_R)$ of Section 3.3 ($\nu = 1/3$ left, $\nu = 0.499$ right.).

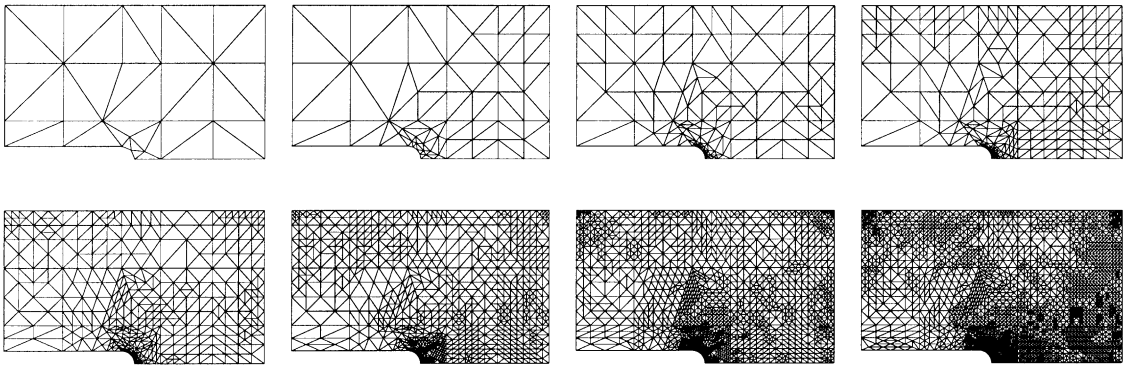

Fig. 10. $\mathscr{T}_0,\ldots,\mathscr{T}_7$ generated by Algorithm $(A^0_{\mathscr{A}})$ in Section 3.3.

$\eta_{\mathscr{A}}$, $\eta_R$ show the same slope and magnitude for $\nu = 0.3$ and $\nu = 0.499$ and so prove to be robust for incompressibility.

## 4. Proofs

Let $u$ solve (2.1)–(2.4) resp. let $u_h$ solve (2.6). Then, define the exact and discrete pressure

$$p := -\lambda \operatorname{div} u \quad \text{and} \quad p_h := -\lambda \operatorname{div}_{\mathscr{T}} u_h \tag{4.1}$$

such that the stress–strain relations read ($\mathbb{1}_{2\times 2}$ denotes the $d \times d$-unit matrix)

$$\sigma = 2\mu\varepsilon(u) - p\mathbb{1}_{2\times 2} \quad \text{and} \quad \sigma_h = 2\mu\varepsilon_{\mathscr{T}}(u) - p_h\mathbb{1}_{2\times 2}. \tag{4.2}$$

For brevity, we define the errors

$$e := u - u_h \in H^1(\mathscr{T})^2 \quad \text{and} \quad \delta := p - p_h \in L^2(\Omega) \tag{4.3}$$

and frequently write $\|\cdot\|_{2,\Omega} := \|\cdot\|_{L^2(\Omega)}$ and $\|\cdot\|_{1,2,\Omega} := \|\cdot\|_{H^1(\Omega)}$ and in this notation even neglect the domain $\Omega$ if there is no risk of confusion.

In the first step of the proof, we consider an auxillary variable to control $\delta$ in the sequel. Notice that we need the extra condition $\int_\Omega \delta \,\mathrm{d}x = 0$ in case $\Gamma = \Gamma_{\mathrm{D}}$. Since $\int_E [u_h]\cdot n_E \,\mathrm{d}s = 0$ for the jump $[u_h]$ of $u_h$ across an interior edge $E \in \mathscr{E}$, $\int_\Omega \delta \,\mathrm{d}x = 0$ is equivalent to $\int_\Gamma (u_{\mathrm{D}} - u_h)\cdot n \,\mathrm{d}s = 0$ and means an extra condition on the choice of $u_h$ on the boundary $\Gamma = \Gamma_{\mathrm{D}}$.

**Lemma 4.1** (Brezzi and Fortin [3], Carstensen and Funken [9]). *If either $\Gamma_{\mathrm{N}}$ has positive surface measure or if $\Gamma_{\mathrm{N}} = \emptyset$ and then $\int_\Gamma (u_{\mathrm{D}} - u_h)\cdot n \,\mathrm{d}s = 0$, there exist a constant $c_7 = c_7(\Omega;\Gamma_{\mathrm{N}})$ and a function $w \in H^1_{\mathrm{D}}(\Omega)$ with*

$$\operatorname{div} w = \delta \quad \text{and} \quad \|w\|_{H^1(\Omega)} \leqslant c_7 \|\delta\| L_{2(\Omega)}. \tag{4.4}$$

Similar to [9,11] we employ $w$ to define some function

$$v := 2\mu c_7^2 e - w \in H^1(\mathscr{T})^2. \tag{4.5}$$

**Lemma 4.2** (Carstensen and Funken [9,11]). *We have*

$$2\mu^2 c_7^2 \|\varepsilon_{\mathscr{T}}(e)\|^2_{L^2(\Omega)} + \left(\frac{1}{2} + 2\mu c_7^2/\lambda\right)\|\delta\|^2_{L^2(\Omega)} \leqslant \int_\Omega (\sigma - \sigma_h) : \varepsilon_{\mathscr{T}} v \,\mathrm{d}x. \tag{4.6}$$

Following [4–7,9] a Helmholtz decomposition of $\varepsilon_{\mathscr{T}}(v)$ allows the split into equilibrium and nonconforming error contributions. Recall $\operatorname{Curl}\beta = (\partial\beta/\partial x_2 - \partial\beta/\partial x_1) \in L^2(\Omega;\mathbb{R}^{d\times 2})$ if $\beta \in H^1(\Omega)^d$ for $d = 1,2$

**Lemma 4.3** (Carstensen and Dolzmann [6], Falk and Morely [15]). *For each $z \in H^1(\mathscr{T})^2$ there exist $\alpha \in H^1_{\mathrm{D}}(\Omega)$ and $\beta \in H^2(\Omega)$ with $(Curl\ Curl\,\beta)n = 0$ on $\Gamma_{\mathrm{N}}$ satisfying*

$$\varepsilon_{\mathscr{T}}(z) = \varepsilon(\alpha) + \mathbb{C}^{-1}\operatorname{Curl}\operatorname{Curl}\beta \quad a.e.\ in\ \Omega. \tag{4.7}$$

The subsequent approximation properties are a key to our reliability proof of the averaging techniques for error control.

**Lemma 4.4** (Carstensen [4], Carstensen and Bartels [5], Carstensen and Verfürth [12]). *There exists a linear mapping $\mathscr{J} : H^1_{\mathrm{D}}(\Omega)^2 \to \mathscr{S}$, bounded if domain and range space are endowed with $H^1$-seminorms, which satisfies*

$$\|h_{\mathscr{T}}^{-1}(\varphi - \mathscr{J}\varphi)\|_{L^2(\Omega)} + \|D\mathscr{J}\varphi\|_{L^2(\Omega)} + \|h_{\mathscr{E}}^{-1/2}(\varphi - \mathscr{J}\varphi)\|_{L^2\left(\bigcup\mathscr{E}\right)} \leqslant c_8\|D\varphi\|_{L^2(\Omega)} \tag{4.8}$$

*for all $\varphi \in H^1_{\mathrm{D}}(\Omega)$. In addition, there holds for all $R \in L^2(\Omega)^2$*

$$\int_\Omega R\cdot(\varphi - \mathscr{J}\varphi)\,\mathrm{d}x \leqslant c_9\|D\varphi\|_{L^2(\Omega)}\left(\sum_{z\in\mathscr{K}} h_z^2 \min_{R_z\in\mathbb{R}^2}\int_{\Omega_z}|R - R_z|^2\,\mathrm{d}x\right)^{1/2}. \tag{4.9}$$

*The positive constants $c_8$, $c_9$ do not depend on the mesh-sizes $h_{\mathscr{T}}$ and $h_{\mathscr{E}}$, but on the shape of the elements only.*

Suppose that in any component and on each edge $E \subset \Gamma_{\mathrm{D}}$, $E \in \mathscr{E}$, the continuous function $u_h - u_{\mathrm{D}}$ has at least one zero on $E$. This assumption is satisfied if for each $j = 1,2$ and $E \in \mathscr{E}_{\mathrm{D}} := \{E \in \mathscr{E}\colon E \subseteq \Gamma_{\mathrm{D}}\}$, we have either $e_j \cdot u_h(z) = e_j \cdot u_{\mathrm{D}}(z)$ for some node $\mathscr{N}_{\mathrm{D}} := \mathscr{N} \cap E$ or $\int_E e_j \cdot (u_h - u_{\mathrm{D}})\,\mathrm{d}s = 0$.

To estimate the error $u_h - u_{\mathrm{D}}$ on the boundary and the incompatibility error we consider the error term

$$\eta_{\mathrm{D}} := \inf\{\|\varepsilon_{\mathscr{T}}(u_h - \eta)\|_{L^2(\Omega)}\colon \eta \in H^1(\Omega)^d,\ \eta = u_{\mathrm{D}}\ \text{on}\ \Gamma_{\mathrm{D}}\}. \tag{4.10}$$

We have the following analogy to [9, Remark 2.1.vii].

**Lemma 4.5.** *There exists $\eta \in H^1(\Omega)^2$ with $\eta = u_{\mathrm{D}}$ on $\Gamma_{\mathrm{D}}$ such that*

$$\eta_{\mathrm{D}} = \|\varepsilon_{\mathscr{T}}(u_h - \eta)\|_{L^2(\Omega)} \leqslant c_{10}\|h_{\mathscr{E}}^{1/2}[\partial_{\mathscr{E}}u_h/\partial s]\|_{L^2\left(\bigcup\mathscr{E}\right)}, \tag{4.11}$$

*where $h_{\mathscr{E}}$ denotes the local edge lengths on $\bigcup\mathscr{E}$ and $\partial_{\mathscr{E}}\cdot/\partial s$ the edgewise tangential derivative. The $h_{\mathscr{E}}$-independent constant $c_{10}$ is independent of $u_{\mathrm{D}}$ and depends only on the aspect ratio of the elements in $\mathscr{T}$.*

**Proof.** The existence and uniqueness of $\eta$ as a weak solution to

$$\operatorname{div}(\varepsilon_{\mathscr{T}}(u_h - \eta)) = 0 \quad \text{in } \Omega, \qquad \varepsilon_{\mathscr{T}}(u_h - \eta)n = 0 \quad \text{on } \Gamma_{\mathrm{N}}, \qquad \text{and} \qquad \eta = u_{\mathrm{D}} \text{ on } \Gamma_{\mathrm{D}} \tag{4.12}$$

follows from the theory of elliptic partial differential equations in linear elasticity. Given $\eta$ we define $\alpha \in H^1_{\mathrm{D}}(\Omega)$ and $\beta \in H^2(\Omega)$ with $(\operatorname{Curl}\operatorname{Curl}\beta)n = 0$ on $\Gamma_{\mathrm{N}}$ satisfying $\varepsilon_{\mathscr{T}}(u_h - \eta) = \mathscr{E}(\alpha) + \operatorname{Curl}\operatorname{Curl}\beta$ similar to Lemma 4.3. Let $b = \operatorname{Curl}\beta$ and notice that $\partial b/\partial s = \operatorname{Curl}\beta n$. Then, integrations by parts and (4.12) show

$$\begin{aligned}\|\varepsilon_{\mathscr{T}}(u_h - \eta)\|_2^2 &= \int_\Omega (D\alpha + \operatorname{Curl}\operatorname{Curl})\,\beta : \varepsilon_{\mathscr{T}}(u_h - \eta)\,\mathrm{d}x = \int_\Omega \varepsilon_{\mathscr{T}}(u_h - \eta) : \operatorname{Curl}\operatorname{Curl}\beta\,\mathrm{d}x \\ &= \int_\Omega D_{\mathscr{T}}(u_h - \eta) : \operatorname{Curl}\operatorname{Curl}\beta\,\mathrm{d}x = \int_\Omega D_{\mathscr{T}}u_h : \operatorname{Curl} b\,\mathrm{d}x - \int_{\Gamma_{\mathrm{D}}} u_{\mathrm{D}}\cdot\operatorname{Curl} bn\,\mathrm{d}s\end{aligned} \tag{4.13}$$

(in the last step we used $\eta = u_D$ on $\Gamma_D$ and $(\operatorname{Curl}\operatorname{Curl}\beta)n = 0$ on $\Gamma_N$). Let $b_h \in \mathscr{S}_1(\mathscr{T})^2$ denote an approximation to $b := \operatorname{Curl}\beta$ as in Lemma 4.4 where the role of the Dirichlet and Neumann boundaries is interchanged: here $\Gamma_N$ acts as the Dirichlet boundary, i.e., $b_h \in C(\bar{\Omega})^2$, $\operatorname{Curl}\beta = b_h$ on $\Gamma_N$. (Recall that $0 = \operatorname{Curl}\operatorname{Curl}\beta n = \partial b/\partial s$ such that $\operatorname{Curl}\beta$ is constant on each component of $\Gamma_N$ and so the interpolation yields indeed $\operatorname{Curl}\beta = b_h$ on $\Gamma_N$.) As in Lemma 4.4 we have

$$\|\operatorname{Curl} b_h\|_2 + \|h_{\mathscr{E}}^{-1/2}(b - b_h)\|_{2,\bigcup\mathscr{E}} + \|h_{\mathscr{T}}^{-1}(b - b_h)\|_2 \leqslant c_{11}\|D^2\beta\|_2. \tag{4.14}$$

Since $\operatorname{Curl} b_h n_E = 0$ on $\Gamma_N$ and, furthermore, $\operatorname{Curl} b_h n_E$ is constant on each $E \in \mathscr{E}$. On interior edges, $[u_h]$ has integral mean zero. This and an elementwise integration by parts show

$$\int_\Omega D_{\mathscr{T}} u_h : \operatorname{Curl} b_h \,\mathrm{d}x = \int_\Gamma u_h \cdot \operatorname{Curl} b_h n_E \,\mathrm{d}s + \sum_{E\in\mathscr{E}} \int_{E\setminus\Gamma} [u_h] \cdot \operatorname{Curl} b_n n_E \,\mathrm{d}s = \int_{\Gamma_D} u_h \cdot \partial b_h/\partial s \,\mathrm{d}s. \tag{4.15}$$

Taking this in (4.13) we deduce with an elementwise integration by parts

$$\begin{aligned}\|\varepsilon_{\mathscr{T}}(u_h - \eta)\|_2^2 &= \int_\Omega D_{\mathscr{T}} u_h : \operatorname{Curl}(b - b_h)\,\mathrm{d}x + \int_{\Gamma_D} \left(u_h \cdot \frac{\partial b_h}{\partial s} - u_D \cdot \frac{\partial b}{\partial s}\right) \mathrm{d}s \\ &= -\int_{\bigcup\mathscr{E}} \left[\frac{\partial u_h}{\partial s}\right] \cdot (b - b_h)\,\mathrm{d}s - \int_{\Gamma_D} \frac{\partial u_D}{\partial s} \cdot (b - b_h)\,\mathrm{d}s \\ &\quad + \int_{\Gamma_D} \left(u_h \cdot \frac{\partial b_h}{\partial s} - u_D \cdot \frac{\partial b}{\partial s}\right) \mathrm{d}s. \end{aligned} \tag{4.16}$$

The boundary $\Gamma$ consists of a finite number of closed Lipschitz curves along which we integrate by parts to obtain

$$\int_\Gamma \frac{\partial u_D}{\partial s} \cdot (b - b_h)\,\mathrm{d}s = -\int_\Gamma u_D \cdot \frac{\partial (b - b_h)}{\partial s}\,\mathrm{d}s. \tag{4.17}$$

With (4.17) in (4.16) we deduce with Cauchy's inequality

$$\begin{aligned}\|\varepsilon_{\mathscr{T}}(u_h - \eta)\|_2^2 &= -\int_{\bigcup\mathscr{E}} \left[\frac{\partial u_h}{\partial s}\right] \cdot (b - b_h)\,\mathrm{d}s + \int_{\Gamma_D} (u_h - u_D) \cdot \frac{\partial b_h}{\partial s}\,\mathrm{d}s \\ &\leqslant \|h_{\mathscr{E}}^{-1/2}(b - b_h)\|_{2,\bigcup\mathscr{E}} \left\| h_{\mathscr{E}}^{1/2} \left[\frac{\partial u_h}{\partial s}\right] \right\|_{2,\bigcup\mathscr{E}} + \|h_{\mathscr{E}}^{-1/2}(u_h - u_D)\|_{2,\Gamma_D} \left\| h_{\mathscr{E}}^{1/2} \frac{\partial b_h}{\partial s} \right\|_{2,\Gamma_D}. \end{aligned} \tag{4.18}$$

Since in each component, $u_h - u_D$ has at least one zero, we deduce

$$\|\bar{u}_h - \bar{u}_D\|_{2,E} \leqslant h_E \left\| \frac{\partial (u_h - \bar{u}_D)}{\partial s} \right\|_{2,E}. \tag{4.19}$$

If $t_E$ denotes the tangential unit vector, $|\partial b_h/\partial s| = |\operatorname{Curl} b_h t_E| \leqslant |\operatorname{Curl} b_h|$. Since $\operatorname{Curl} b_h$ is constant on each element $T \in \mathscr{T}$, we have with $h_E^2 \leqslant c_{12}|T|$ that

$$h_E \left\| \frac{\partial b_h}{\partial s} \right\|_{2,E}^2 \leqslant c_{12}\|\operatorname{Curl} b_h\|_{2,E}^2. \tag{4.20}$$

Involving (4.19) and (4.20) in (4.18), we infer from (4.14) that

$$\|\varepsilon_{\mathscr{T}}(u_h - \eta)\|_2^2 \leqslant c_{11}\|D^2\beta\|_2 \left( \left\| h_{\mathscr{E}}^{1/2} \left[\frac{\partial u_h}{\partial s}\right] \right\|_{2,\bigcup\mathscr{E}} + c_{12} \left\| h_{\mathscr{E}}^{1/2} \frac{\partial (u_h - u_D)}{\partial s} \right\|_{2,\Gamma_D} \right). \tag{4.21}$$

With $L^2$-orthogonality of $\mathscr{E}(\alpha)$ and Curl Curl $\beta$ we have

$$\|D^2\beta\|_2 = \|\mathrm{Curl}\ \mathrm{Curl}\,\beta\|_2 \leqslant \|\varepsilon_{\mathscr{T}}(u_h-\eta)\|_2 = \eta_{\mathrm{D}},$$

whence a division of (4.12) by $\|D^2\beta\|_2$ shows the assertion with $(u_h-u_{\mathrm{D}})|_{\Gamma_{\mathrm{D}}} = [u_h]|_{\Gamma_{\mathrm{D}}}$. □

**Proof of Theorem 2.1.** With (4.5) and $\eta$ as in Lemma 4.5, set $z := 2\mu c_7^2(u-\eta) - w \in H^1_{\mathrm{D}}(\Omega)$. Then, Lemma 4.5 and $\|\sigma-\sigma_h\|_2 \leqslant \|2\mu\varepsilon(e)\|_2 + \|\delta\|_2$ shows

$$\begin{aligned}\int_\Omega (\sigma-\sigma_H) : \varepsilon_{\mathscr{T}}(v)\,\mathrm{d}x &= 2\mu c_7^2 \int_\Omega (\sigma-\sigma_h) : \varepsilon_{\mathscr{T}}(\eta-u_h)\,\mathrm{d}x + \int_\Omega (\sigma-\sigma_h) : \varepsilon(z)\,\mathrm{d}x \\ &\leqslant 2\mu c_7^2 c_{10}\eta_{\mathrm{D}}(\|2\mu\varepsilon(e)\|_2 + \|\delta\|_2) + \int_\Omega (\sigma-\sigma_h) : \varepsilon(z-\mathscr{J}z)\,\mathrm{d}x \end{aligned} \tag{4.22}$$

because $\int_\Omega (\sigma-\sigma_h) : \varepsilon(\mathscr{J}z)\,\mathrm{d}x = 0$ owing to the Galerkin property from (2.1), (2.2) and (2.6) for $v_h = \mathscr{J}z \in \mathscr{S}$. This and Lemma 4.2 show

$$\|2\mu\varepsilon(e)\|^2_{L^2(\Omega)} + \|\delta\|^2_{L^2(\Omega)} \leqslant c_{13}\left(\eta_{\mathrm{D}} + \int_\Omega (\sigma-\sigma_h) : \varepsilon_{\mathscr{T}}(z-\mathscr{J}z)\,\mathrm{d}x\right) \tag{4.23}$$

and it remains to analyze the last integral in (4.23). This term arose in the context of conforming estimates in Part II [11] and can be estimated by standard arguments as an elementwise integration by parts and (4.8) but also (4.9). We refer to [11] and omit the details. □

**Proof of Theorem 2.2.** With $\mathrm{div}_{\mathscr{T}}\sigma_h = 0$ we can employ (4.9) to estimate the term $\int_\Omega f\cdot(z-\mathscr{J}z)\,\mathrm{d}x$ that arises after an integration by parts in the last integral in (4.23). We refer to [12,4] for more details (in case of the Laplace operator) and omit them here. □

Suppose for each edge $E \in \mathscr{E}_{\mathrm{D}}$ and each component $j = 1,2$ that the function $e_j\cdot(u_h-u_{\mathrm{D}})$ has either integral mean zero or vanishes at the endpoints of $E$ and suppose that $u_{\mathrm{D}} \in H^2(\mathscr{E}_{\mathrm{D}})$, i.e., $u_{\mathrm{D}}|_E$ is in $H^2(E)$ for each edge $E \in \mathscr{E}_{\mathrm{D}}$.

**Lemma 4.6.** *The function $\eta \in H^1(\Omega)^2$ with $\eta = u_{\mathrm{D}}$ on $\Gamma_{\mathrm{D}}$ from Lemma 4.5 satisfies*

$$\begin{aligned}\eta_{\mathrm{D}} = \|\varepsilon_{\mathscr{T}}(u_h-\eta)\|_{L^2(\Omega)} &\leqslant c_{14}\|h_{\mathscr{E}}^{3/2}\partial^2_{\mathscr{E}}u_{\mathrm{D}}/\partial s^2\|_{L^2(\Gamma_{\mathrm{D}})} \\ &\quad + c_{15}\left(\|D_{\mathscr{T}}u_h - Q\|_2 + \left\|h_{\mathscr{E}}^{1/2}\left(\frac{\partial u_{\mathrm{D}}}{\partial s} - Qt_E\right)\right\|_{2,\Gamma_{\mathrm{D}}}\right)\end{aligned} \tag{4.24}$$

*for all $Q \in \mathscr{S}^1(\mathscr{T})^{2\times 2}$. The $h_{\mathscr{E}}$-independent constants $c_{14},\ c_{15}$ are independent of $u_{\mathrm{D}}$ and depend only on the aspect ratio of the elements in $\mathscr{T}$.*

**Proof.** Let $Q \in S^1(\mathscr{T})^{2\times 2}$, $b_h$ and $b$ as in the proof of Lemma 4.5 (4.16) therein to see with an integration by parts over $\Omega$

$$\begin{aligned}\eta_{\mathrm{D}}^2 &= \int_\Omega D_{\mathscr{T}}u_h : \mathrm{Curl}\,(b-b_h)\,\mathrm{d}x + \int_{\Gamma_{\mathrm{D}}}\left(u_h\cdot\frac{\partial b_h}{\partial s} - u_{\mathrm{D}}\cdot\frac{\partial b}{\partial s}\right)\mathrm{d}s \\ &= \int_\Omega (D_{\mathscr{T}}u_h - Q) : \mathrm{Curl}\,(b-b_h)\,\mathrm{d}x + \int_\Omega Q : \mathrm{Curl}(b-b_h)\,\mathrm{d}x + \int_{\Gamma_{\mathrm{D}}}\left(u_h\cdot\frac{\partial b_h}{\partial s} - u_{\mathrm{D}}\cdot\frac{\partial b}{\partial s}\right)\mathrm{d}s \\ &\leqslant \|D_{\mathscr{T}}u_h - Q\|_2\|\mathrm{Curl}(b-b_h)\|_2 - \int_\Omega \mathrm{Curl}\,Q\cdot(b-b_h)\,\mathrm{d}x + \int_{\Gamma_{\mathrm{D}}}\left(\frac{\partial u_{\mathrm{D}}}{\partial s} - Qt_E\right)\cdot(b-b_h)\,\mathrm{d}s \\ &\quad - \int_{\Gamma_{\mathrm{D}}}\frac{\partial u_{\mathrm{D}}}{\partial s}\cdot(b-b_h)\,\mathrm{d}s + \int_{\Gamma_{\mathrm{D}}}\left(u_h\cdot\frac{\partial b_h}{\partial s} - u_{\mathrm{D}}\cdot\frac{\partial b}{\partial s}\right)\mathrm{d}s,\end{aligned} \tag{4.25}$$

where we utilized $b = b_h$ on $\Gamma_N$. The last two integrals in (4.25) are analyzed as in Lemma 4.5. Let $\bar{u}_h$ and $\bar{u}_D$ be the edgewise integral mean of $u_h$ and $u_D$, respectively. Then, since $\partial b_h/\partial s$ is constant on each edge, we have

$$
\begin{aligned}
&-\int_{\Gamma_D} \frac{\partial u_D}{\partial s} \cdot (b - b_h)\,\mathrm{d}s + \int_{\Gamma_D} \left( u_h \cdot \frac{\partial b_h}{\partial s} - u_D \cdot \frac{\partial b}{\partial s} \right) \mathrm{d}s \\
&\quad = \int_{\Gamma_D} (\bar{u}_h - \bar{u}_D) \cdot \frac{\partial b_h}{\partial s}\,\mathrm{d}s \leqslant c_{12}^{1/2} \|\mathrm{Curl}\, b_h\|_{2,E} \|h_{\mathscr{E}}^{-1/2}(\bar{u}_h - \bar{u}_D)\|_{2,\Gamma_D}.
\end{aligned} \tag{4.26}
$$

By assumption, for $E \in \mathscr{E}_D$ and $j = 1, 2$, the function $e_j \cdot (\bar{u}_h - \bar{u}_D)$ is either zero or $e_j \cdot (u_h - u_D)$ vanishes at the endpoints of $E$. In the latter case, a standard estimate shows

$$
\|e_j \cdot (\bar{u}_h - \bar{u}_D)\|_{2,E} \leqslant \|e_j \cdot (u_h - u_D)\|_{2,E} \leqslant h_E^2 \|\partial^2 u_D/\partial s^2\|_{2,E}. \tag{4.27}
$$

The second term on the right-hand side in (4.25) that involves the integrand $(\mathrm{Curl}\, Q) \cdot (b - b_h) = (\mathrm{Curl}_{\mathscr{T}}(Q - D_{\mathscr{T}} u_h)) \cdot (b - b_h)$ requires an inverse estimate

$$
\|\mathrm{Curl}_{\mathscr{T}}(Q - D_{\mathscr{T}} u_h)\|_{2,T} \leqslant c_{16} h_T^{-1} \|Q - D_{\mathscr{T}} u_h\|_{2,T} \tag{4.28}
$$

(recall that $Q - D_{\mathscr{T}} u_h$ is affine on $T \in \mathscr{T}$). Employing (4.26)–(4.28), Cauchy's inequality, and the stability and approximation properties (4.14), we deduce in (4.25) that

$$
\begin{aligned}
\eta_D^2 &\leqslant \|D_{\mathscr{T}} u_h - Q\|_2 \|\mathrm{Curl}(b - b_h)\|_2 + \|h_{\mathscr{T}} \mathrm{Curl}(Q - D_{\mathscr{T}} u_h)\|_2 \|h_{\mathscr{T}}^{-1}(b - b_h)\|_2 \\
&\quad + \left\| h_{\mathscr{E}}^{1/2} \left( \frac{\partial u_D}{\partial s} - Q t_E \right) \right\|_{2,\Gamma_D} \left\| h_{\mathscr{E}}^{1/2}(b - b_h) \right\|_{2,\Gamma_D} + c_{12}^{1/2} \|\mathrm{Curl}\, b_h\|_2 \|h_{\mathscr{E}}^{3/2} \partial_{\mathscr{E}}^2 u_D/\partial s^2\|_{2,\Gamma_D} \\
&\leqslant \|D^2 \beta\|_2 \left( c_{14} \|h_{\mathscr{E}}^{3/2} \partial_{\mathscr{E}}^{3/2} u_D/\partial s^2\|_{2,\Gamma_D} + c_{15} \|D_{\mathscr{T}} u_h - Q\|_2 + c_{15} \left\| h_{\mathscr{E}}^{1/2} \left( \frac{\partial u_D}{\partial s} - Q t_E \right) \right\|_{2,\Gamma_D} \right)
\end{aligned} \tag{4.29}
$$

from which the assertion is concluded as in Lemma 4.5. □

**Proof of Theorem 2.3.** We start as in the Proof of Theorem 2.1 and consider (4.23) where we employ Lemma 4.6 to estimate $\eta_D$. The remaining term is estimated in Part II [11] where we showed that

$$
\int_\Omega (\sigma - \sigma_h) : \varepsilon_{\mathscr{T}}(z - \mathscr{J} z)\,\mathrm{d}x \leqslant c_{17} \|Dz\|_2 \Big( \|\sigma_h - \sigma^*\|_{L^2(\Omega)} + \|h_{\mathscr{E}}^{3/2} \partial_{\mathscr{E}} g/\partial s\|_{L^2(\Gamma_N)} + \|h_{\mathscr{T}}^2 Df\|_{L^2(\Omega)} \Big). \tag{4.30}
$$

As in Part II [11] we bound $\|Dz\|_2$ with Korn's inequality by $\|2\mu\varepsilon(e)\|_{L^2(\Omega)} + \|\delta\|_{L^2(\Omega)} + \eta_D$ (up to a constant factor) and finish the proof as in [11]. □

Then, let $\mathscr{N}^*$ denote the set of all nodes which are either free or belong to two aligned edges in $\mathscr{E}_D$. In case $z \in \mathscr{N}^*$ is a free node, $\Omega_z = \omega_z := \mathrm{interior}(\bigcup\{T \in \mathscr{T} : z \in T\})$ denotes the patch of $z$ and otherwise $\Omega_z = \omega_z \bigcup \omega_\zeta$ is the union of two neighboring patches where $\zeta$ is a neighboring node such that $\mathrm{conv}\{z, \zeta\} = E \in \mathscr{E}$ and either $\zeta$ is an interior node or $E$ is not parallel to the $x_1$-axis. For each $z \in \mathscr{N}^*$, let $\mathscr{T}_z := \mathscr{T}|_{\Omega_z} := \{T \in \mathscr{T} : T \subset \bar{\Omega}_z\}$ denote the (local) triangulation on the extended patch $\Omega_z$.

We need the following lemma with $v_h = 0 \in \mathscr{S}_D^1(\mathscr{T}_z) := \{V \in \mathscr{S}^1(\mathscr{T}_z)^2 : V = 0 \text{ on } \gamma_z\}$ from [9] (where $\gamma_z := \{E_1, E_2\}$ if $E_1, E_2 \in \mathscr{E}_D$ are two distinct aligned edges (cf. the definition of $\mathscr{N}^*$ if $z \in \Gamma_D$) and $\gamma_z := \emptyset$ if $z$ is a free node). Let $\mathscr{E}_z := \{E \in \mathscr{E} : z \in E\}$.

**Lemma 4.7** (Carstensen and Funken [9]). *For any $z \in \mathscr{N}^*$ there exists a h-independent constant $c_{18} > 0$ such that, for all $w_h \in \mathscr{W} = \mathscr{W}_1 \times \mathscr{W}_2$,*

$$\left(\sum_{E\in\mathscr{E}_z} h_E\|[\partial w_h/\partial s]\|^2_{L^2(E)}\right)^{1/2} \leqslant c_{18}\left(\|h_{\mathscr{E}}^{3/2}\partial^2(u_{\mathrm{D}}-\mathscr{I}u_{\mathrm{D}})/\partial s^2\|_{L^2(\Gamma_{\mathrm{D}}\cap\partial\Omega_z)} + \min_{(v_h,\mathscr{T}_h)\in\mathscr{S}^1_{\mathrm{D}}(\mathscr{T}_z)\times\mathscr{S}^1(\mathscr{T}_z)^{2\times 2}}\|\varepsilon_{\mathscr{T}}(w_h-v_h)-\tau_h\|_{L^2(\Omega_z)}\right). \tag{4.31}$$

**Proof of Theorem 2.4.** We start as in the Proof of Theorem 2.1 and consider (4.23) where we employ Lemma 4.5 to estimate $\eta_{\mathrm{D}}$. The remaining terms are estimated as in the previous proof and so we obtain

$$\|2\mu\varepsilon_{\mathscr{T}}(u-u_h)\|_2+\|\lambda\mathrm{div}_{\mathscr{T}}(u-u_h)\|_2 \leqslant c_{19}\Big(\eta_Z+\|h_{\mathscr{E}}^{1/2}[\partial_{\mathscr{E}}u_h/\partial s]\|_{2,\bigcup\mathscr{E}}+\|h_{\mathscr{E}}^{3/2}\partial^2_{\mathscr{E}}u_{\mathrm{D}}/\partial s^2\|_{2,\Gamma_{\mathrm{D}}} + \|h_{\mathscr{E}}^{3/2}\partial_{\mathscr{E}}g/\partial s\|_{2,\Gamma_{\mathrm{D}}}+\|h^2_{\mathscr{T}}Df\|_2\Big). \tag{4.32}$$

Hence, if suffices to prove

$$\|h_{\mathscr{E}}^{1/2}[\partial_{\mathscr{E}}u_h/\partial s]\|_{2,\bigcup\mathscr{E}} \leqslant c_{20}(\eta_Z+\|h_{\mathscr{E}}^{3/2}\partial^2_{\mathscr{E}}u_{\mathrm{D}}/\partial s^2\|_{L^2,(\Gamma_{\mathrm{D}})}). \tag{4.33}$$

By construction of $\mathscr{N}^*$ and the assumptions of the mesh, each edge $E$ belongs to $\mathscr{E}_z$ for at least one $z\in\mathscr{N}^*$. Lemma 4.7 then shows (with $w_h=u_h,\ v_h=0$, and $\tau_h:=\mathbb{C}^{-1}\sigma_h^*|_{\Omega_z}$)

$$c_{18}^{-1}h_E^{1/2}\|[\partial u_h/\partial s]\|^2_{2,E} \leqslant \|h_{\mathscr{E}}^{3/2}\partial^2(u_{\mathrm{D}}-\mathscr{I}u_{\mathrm{D}})/\partial s^2\|_{2,\Gamma_{\mathrm{D}}\cap\partial\Omega_z}+\|\varepsilon_{\mathscr{T}}(u_h)-\mathbb{C}^{-1}\sigma_h^*\|_{2,\Omega_z}. \tag{4.34}$$

The material law (2.5) shows $|\varepsilon_{\mathscr{T}}(u_h)-\mathbb{C}^{-1}\sigma_h^*|=|\mathbb{C}^{-1}(\sigma_h-\sigma_h^*)|\leqslant c_{21}|\sigma_h-\sigma_h^*|$ for some $\lambda$-independent constant $c_{21}$ (assuming $\lambda\to\infty$ and so that $\lambda$ is greater than a fixed positive constant) that depends on $\mu>0$. Utilizing this in (4.34) and summing over all $E$ we obtain (4.33) since the patches $\Omega_z$ have a finite overlap only and the number of edges that are related to one $z\in\mathscr{N}^*$ is bounded. □

## References


[1] W. Bao, J.W. Barrett, A priori and a posteriori error bounds for a non-conforming linear finite element approximation of a non-Newtonian flow, M²AN 32 (1998) 843–858.

[2] S. Bartels, C. Carstensen, S. Jansche, A posteriori error estimates and adaptive mesh-refining for non-conform finite element methods, Berichtsreihe des Mathematischen Seminars Kiel, Technical report 97-8, Universität Kiel, 1997 (revised version).

[3] F. Brezzi, M. Fortin, Mixed and Hybrid Finite Element Methods, Springer, Berlin, 1991.

[4] C. Carstensen, Quasi interpolation and a posteriori error analysis in finite element method, M²AN 33 (1999) 1187–1202.

[5] C. Carstensen, S. Bartels, Each averaging technique yields reliable a posteriori error control in FEM on unstructured grids. Part I. Low order conforming, nonconforming, and mixed FEM, Berichtsreihe des Mathematischen Seminars Kiel, Technical report 99-11, Christian-Albrechts-Universität zu Kiel, Kiel, 1999 (http://www.numerik.uni-kiel.de/reports/1999/99-11.html).

[6] C. Carstensen, G. Dolzmann, A posteriori error estimates for mixed FEM in elasticity, Numer. Math. 81 (1998) 187–209.

[7] C. Carstensen, G. Dolzmann, S.A. Funken, D. Helm, Locking-free adaptive mixed finite element methods in elasticity, Comput. Methods Appl. Mech. Engrg. 190 (2000) 1701–1718.

[8] C. Carstensen, S.A. Funken, Constants in Clément-interpolation error and residual based a posteriori error estimates in finite element methods, East-West Numer. Anal. 8 (2000) 153–256.

[9] C. Carstensen, S.A. Funken, A posteriori error control in low-order finite element discretisations of incompressible stationary flow problems, Math. Comp. 70 (2001) 1353–1381.

[10] C. Carstensen, S.A. Funken, Averaging technique for FE-a posteriori error control in elasticity. Part I: Conforming FEM, Comput. Methods Appl. Mech. Engrg. 190 (2001) 1.

[11] C. Carstensen, S.A. Funken, Averaging technique for FE-a posteriori error control in elasticity. Part II: Locking-free FEM, Comput. Methods Appl. Mech. Engrg. 190 (2001) 4663–4675.

[12] C. Carstensen, R. Verfürth, Edge residuals dominate a posteriori error estimates for low order finite element methods, SIAM J. Numer. Anal. 36 (1998) 1571–1587.

[13] P.G. Ciarlet, The Finite Element Method for Elliptic Problems, North-Holland, Amsterdam, 1978.

[14] E. Dari, R. Duran, C. Padra, V. Vampa, A posteriori error estimators for noncomforming finite element methods, Math. Modelling Numer. Anal. 30 (1996) 385–400.

[15] R.S. Falk, M. Morely, Equivalence of finite element methods for problems in elasticity, SIAM J. Numer. Anal. 27 (1990) 1486–1505.
[16] L. Hörmander, Linear Partial Differential Operators, Springer, Berlin, 1963.
[17] R. Kouhia, R. Stenberg, A linear nonconforming finite element method for nearly incompressible elasticity and Stokes flow, Comput. Methods Appl. Mech. Engrg. 124 (1995) 195–212.
[18] J.L. Lions, E. Magenes, Non-homogeneous Boundary Value Problems and Applications, vol. I, Springer, Berlin, 1972.
[19] R. Stenberg, A family of mixed finite elements for the elasticity problem, Numer. Math. 53 (1998) 513–538.